

Enhancing the Inhibition Effect and Adsorption Efficiency of Ethoxylated Dodecyl Alcohols on Corrosion of 316 Stainless Steels in 2M HCl

M. Abdallah^{1,2,*}, M. Alfakeer³, Arej S Al-Gorair³, A. Al Bahir⁴, M. Sobhi^{2,5}

¹ Chem. Depart. Faculty of Appl. Sci., Umm Al-Qura Univ., Makkah, Saudi Arabia

² Chem. Depart. Faculty of Sci, Benha Univ., Benha, Egypt

³ Chem. Depart., College of Sci., Princess Nourah bint Abdulrahman Univ., Riyadh, Saudi Arabia

⁴ Chem. Depart. Faculty of Sciences, King Khalid Univ., Abha, Saudi Arabia

⁵ Chem. Depart. Faculty of Sci., Tabuk University, Tabuk, Saudi Arabia

*E-mail: metwally555@yahoo.com

Received: 6 February 2021 / Accepted: 26 March 2021 / Published: 30 April 2021

The inhibiting impact of three molecules of ethoxylated dodecyl alcohols (EDA) with different ethylene oxide units against the corrosion of 316 stainless steel (316SS) in 2M HCl solutions was examined. Electrochemical tests such as galvanostatic, potentiodynamic anodic polarization and electrochemical impedance spectroscopy were applied to assign the electrochemical parameters. All the tests used confirm the inhibitory action of EDA molecules. The inhibition efficacy increasing with increasing the concentrations of EDA molecules, increase of ethylene oxide units and reducing at elevated temperature. The inhibition was expounded by the forming of adsorbed film on the surface 316SS through the EO unit while the hydrocarbon parts protrude brush-like into the solution. This adsorption obeyed Temkin's isotherm. Galvanostatic polarization demonstrates that the EDA molecules act as mixed inhibitors. The thermodynamic kinetics parameters for activation processes were determined and expounded. EDA molecules reduces the pitting attack of 316SS in NaCl solution from the transmitting of the pitting potential to the noble trend.

Keywords: Ethoxylated dodecyl alcohols, 316 stainless steel, Inhibitors, Pitting, Adsorption, SEM.

1. INTRODUCTION

Stainless steel alloy Type 316 (316SS) is utilized in many strategic industries such as chemical, processing, oil and gas, tanks, pipes, pumps, and many industries. This is because it has great resistance to corrosion due to its excellent thermal and mechanical properties. It contains elements such as Cr, Ni, Fe and Mo, and the presence of these elements leads to the forming of a layer containing oxides of these

elements on the surface and thus reduces the rate of corrosion of this alloy in aqueous solutions [1]. HCl solutions are applied in the chemical cleaning and pickling processes of stainless steel with high efficacy. But it is unfortunate that it causes corrosion [2]. Therefore, scientists have tended to solve this problem by using corrosion inhibitors to preserve this alloy and extend its life for as long as possible.

The utilization of corrosion inhibitors is an efficacious way to diminish the corrosion of 316SS. Most of these inhibitors are either inorganic or organic compounds involving some hetero atoms and contain several bonds and aromatic rings that serve to adsorb them on the SS surface [3-14]. The efficacy of the inhibitor depends on the chemical formula of the anticorrosive used and the existence of some electro donating or expelling groups in its structure, characteristics of the corrosive media, the type of SS surface, and the electrochemical voltage at interface [15].

It is known that these compounds give high inhibitory effectiveness, but unfortunately, it is harmful to the environment and human health, and therefore, this study is based on the use of inexpensive and environmentally friendly surfactant molecules as anti-corrosion of 316SS in a 2M HCl solution. In previous studies, surfactant molecules have been used as corrosion inhibitor for steel in acidic media [16-19].

The main target of this manuscript is to use of three molecules of ethoxylated dodecyl alcohols (EDA) with different amount of ethylene oxide to minimize the dissolution of 316 SS in 2M HCl solution. Electrochemical tests such as, galvanostatic polarization (GAP), potentiodynamic anodic polarization (PDAP) and electrochemical impedance spectroscopy (EIS) are utilized in this manuscript to measure the inhibitory efficacy of EDA molecules. The adsorption isotherm and the activation thermodynamic parameters were also investigated.

2. EXPERIMENTAL TESTS

2.1. 316 stainless steel (316 SS)

The chemical composition of 316 SS utilized in this manuscript are: (wt. %) C 0.024, Cr 17.02, Ni 12.05, Mn 1.30, P 0.045, S 0.02, Si 0.44, Mo 2.04 and the rest is Fe

2.2. Electrochemical tests

For electrochemical tests, a 316SS cylindrical rod immersed in Araldite with an exposed surface area of 0.52 cm^2 was applied in this research. The electrochemical cell was utilized in these tests including three holes containing working 316SS electrode, a saturated calomel electrode (SCE) and Pt electrode. Before any tests the electrode was cleaned by abraded with some grade of sand paper reached to 1500 grade and washed with distilled water and acetone. Finally dried by filter paper, all tested solutions were prepared using double distilled water. The tests were performed at $27 \pm 0.5 \text{ }^\circ\text{C}$ using a super-circulating thermostat

Galvanostatic polarization (GAP) and potentiodynamic anodic polarization (PDAP) were performed at scanning rate 5mVs^{-1} and 1mVs^{-1} , respectively. The potential of the working electrode was controlled by PS6 Meinsberger potentiostat/ galvanostat, the current density- potential curves recorded on PC using special programme.

The electrochemical impedance spectroscopy (EIS) tests were achieved using a potentiostat-controlled computer (Auto-Lab 30, Metrohm). The EIS experiment was performed with AC signals of 5 mV peak-to-peak at open circuit potential in the frequency range of 100 kHz to 10 mHz.

2.3. Scanning Electron Microscope

A scanning electron microscope (SEM) model T-200 was utilized to assay the surface morphology of the surface of 316SS in a free 2MHCl solution and in the presence of 225ppm of three molecules of EDA. All images of the corroded specimens were taken with magnification ($\times 500$). All tested samples were immersed in the examined solutions after being exposed to GAP tests. After the surface handling the samples were stocked in a dryer until they were examined.

2.4. Inhibitor used

Ethoxylated dodecyl alcohol molecule (EDA) were prepared as explained previously [20], and having the formula: $\text{C}_{12}\text{H}_{26}\text{O}(\text{C}_2\text{H}_4\text{O})_z\text{H}$

where z is the amount of ethylene oxide (EO) and equal to 6, 8 and 10 for the three molecules EDA1, EDA2 and EDA3, respectively

IUPAC name of EDA1 molecule is: 3,6,9,12,15,18-hexaoxatriacontan-1-ol.

IUPAC name of EDA2 molecule is: 3,6,9,12,15,18,21,24-octaoxahexatriacontan-1-ol.

IUPAC name of EDA3 molecule is: 3,6,9,12,15,18,21,24,27,30-decaoxadotetracontan-1-ol.

3. RESULTS AND DISCUSSION

3.1. Galvanostatic polarization tests

Fig.1 elucidates the GAP curves of 316 SS in free 2MHCl solutions and involving some concentrations of EDA3 as an example of the investigated EDA. Analogous curves for EDA1 and EDA2 molecules are obtained but not shown. Some corrosion parameters e.g., anodic and cathodic Tafel slopes (β_a & β_c), corrosion current density (I_{corr}) achieved from the extrapolation of the anodic and cathodic polarization curves with corrosion potential (E_{corr}), surface coverage (θ) and inhibition efficacy (%P) were deduced from the GAP curves and included in Table 1. The values of %P and θ were determined from the following equations:

$$\% P = \left[1 - \frac{I_{\text{corr.in}}}{I_{\text{corr.f}}} \right] 100 \quad (1)$$

$$\theta = \left[1 - \frac{I_{\text{corr.in}}}{I_{\text{corr.f}}} \right] \quad (2)$$

where, $I_{corr,f}$ and $I_{corr.in}$ are the corrosion current densities for 316SS in free HCl and with EDA molecules .

From the GAP curves and parameters that occurred in Table1, it is obvious that the anodic reaction of 316 SS and reduction hydrogen evolution were inhibited upon addition of EDA molecules and this inhibition was clearer with increasing EDA concentration. Also, the anodic and cathodic Tafel lines are transferred to more positive and negative potentials with respect to the free curve. This indicates that the EDA molecules act as mixed inhibitors [21]. The values of both β_c and β_a of the investigated EDA molecules were slightly moved to more negative or more positive potentials demonstrating that, these molecules acted as mixed inhibitors. This means that, the EDA molecules blocked both the cathodic and anodic sites without altering the corrosion mechanism [22].

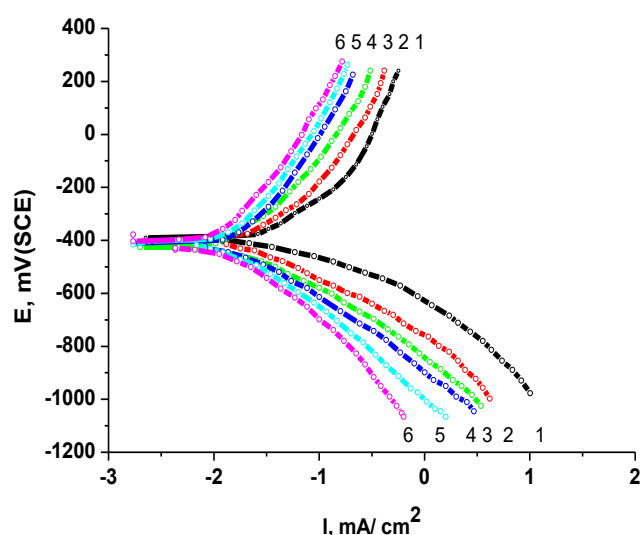


Figure 1. GAP curves of 316 SS in free 2 M HCl solution and containing certain concentrations of the EDA3 at 300 °K; 1) 0.00 ppm EDA3 2) 0.25 ppm EDA3 3) 0.75 ppm EDA3 4) 125 ppm EDA3 5) 175 ppm EDA3 6) 225 ppm EDA3

The values of E_{corr} are changed slightly with increasing concentrations EDA molecules and no significant potential shift is noticed, and this demonstrates the mixed inhibitor action. The values of I_{corr} are lowered and the values of %P and θ are increases confirm the inhibitory strength of the EDA molecules. The % P ranking of the three EDA molecules decreases in the following sequence: EDA3 > EDA2 > EDA1. The % P values raise parallels with increment the amount of the ethylene oxide unit. The inhibitory strength of EGA molecules was interpreted by obscure the 316SS surface by adsorbing its molecules through the active centers present in their structures.

Table 1. Corrosion parameters determined from GAP of 316 SS in free 2MHCl solution and involving some concentrations of EDA molecules at 300°K

EDA Concentration	β_a , mV dec ⁻¹	$-\beta_c$ mV dec ⁻¹	$-E_{corr}$, V(SCE)	I_{corr} .mA cm ⁻²	θ	%P
2MHCl	130	142	405	0.132	-	-
<u>2MHCl + EDA 1</u>						
25 ppm	134	148	405	0.042	0.682	68.18
75 ppm	138	152	407	0.036	0.727	72.72
125 ppm	144	155	410	0.028	0.788	78.78
175 ppm	140	157	414	0.020	0.848	84.84
225ppm	145	160	418	0.012	0.909	90.90
<u>2MHCl + EDA 2</u>						
25 ppm	138	146	402	0.039	0.705	70.45
75 ppm	141	148	409	0.027	0.795	79.54
125 ppm	144	152	411	0.022	0.833	83.33
175 ppm	148	155	415	0.015	0.886	88.63
225ppm	146	158	419	0.010	0.924	92.42
<u>2MHCl + EDA 3</u>						
25 ppm	140	154	408	0.035	0.735	73.48
75 ppm	142	158	410	0.024	0.818	81.82
125 ppm	148	160	415	0.017	0.871	87.12
175 ppm	150	164	418	0.012	0.909	90.91
225ppm	1146	168	422	0.008	0.939	93.94

3.2. Impact of temperature

The impact of elevated temperature on GAP of 316 SS was inspected in blank 2M HCl solution and upon inclusion 225ppm of three EDA molecules. Analogous curves to Fig.1 are obtained but not shown. The corrosion parameters such as I_{corr} . and %P was determined and recorded in Table 2. From the data presented in this figure, it is apparent that, with increasing temperature, the values of I_{corr} . increases and the values of %P lowered indicating the inhibition action of EDA molecules reduced with elevated temperature. This demonstrates that the adsorption of EDA on the surface of 316 SS is physical.

The activation kinetics parameters such as, activation energy (E_a), enthalpy of activation(ΔH^*) and entropy of activation ΔS^* for the corrosion of 316 SS in free 2MHCl solution and when containing 225 ppm of EDA molecules were determined by applying Arrhenius and transition state equation [23,24]:

$$\frac{R_{corr}}{A} = \exp\left(\frac{-E_a^*}{RT}\right) \tag{3}$$

$$\ln\left(\frac{N_A h R_{corr}}{RT}\right) = \frac{\Delta S^*}{RT} - \frac{\Delta H^*}{RT} \tag{4}$$

where, R_{corr} is the rate of corrosion and is related to corrosion current density I_{corr} [25], A is the frequency factor, N_A is Avogadro’s number and R is gas constant and T is the absolute temperature.

Table 2. Impact of elevated temperature on the values of I_{corr} and %P for corrosion of 316 SS in 2MHCl and containing 225ppm of EDA molecules

Comp.	T, K	I_{corr} -mA cm ⁻²	%P
2MHCl	300	0.132	-
	310	0.165	-
	320	0.192	-
	330	0.212	-
2MHCl + 225ppm EDA1	300	0.012	90.90
	310	0.028	83.03
	320	0.048	75.00
	330	0.062	70.75
2MHCl + 225ppm EDA2	300	0.010	92.42
	310	0.021	87.27
	320	0.040	79.16
	330	0.055	74.06
2MHCl + 225ppm EDA3	300	0.008	93.94
	310	0.018	86.36
	320	0.035	81.77
	330	0.048	77.36

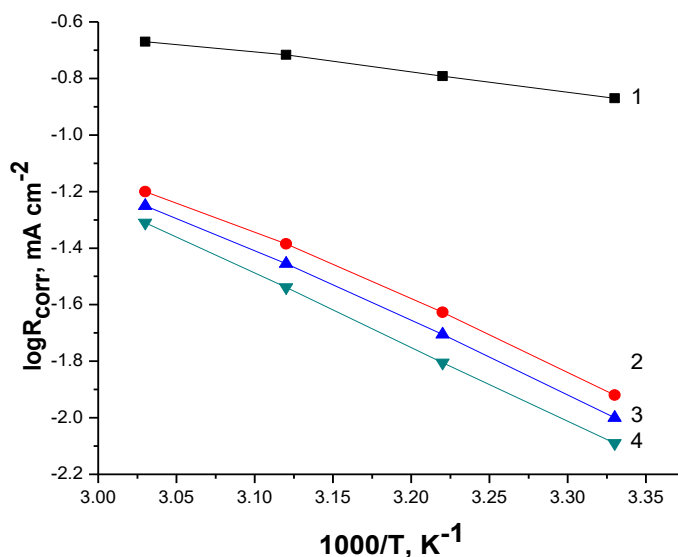


Figure 2. Arrhenius plots of 316 SS in 2 M HCl solution and the presence of 225 ppm of: EDA molecules; 1) free 2MHCl 2) EDA1 3) EDA2 4) EDA3

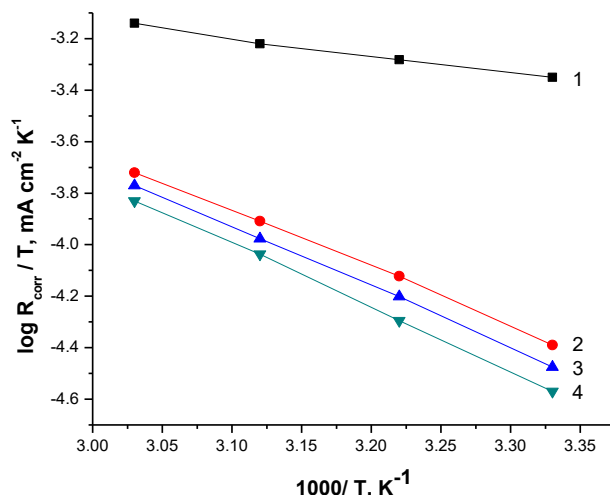


Figure 3. Transition state plots of 316 SS in 2 M HCl solution and the presence of 225 ppm of: EDA molecules 1) free 2MHCl 2) EDA1 3) EDA2 4) EDA3

Fig.2 displays the plots of $\log R_{corr}$ versus $1/T$ for 316 SS in free 2MHCl solution and when including 225 ppm of three EDA molecules. Straight lines were acquired. The values of E_a^* were determined from the slopes of straight lines ($-E_a^*/2.303R$) and equals to $28.72 \text{ KJ mol}^{-1}$ in free 2M HCl and equal to $38.65, 42.12$ and $44.03 \text{ KJ mol}^{-1}$ for molecules EDA1, EDA2 and EDA3 respectively

It is observed that, the presence of EDA molecules increases, the values of E_a^* increases than in the free 2MHCl solution. This demonstrated that the adsorption of EDA molecules on the 316SS surface through the formation of barrier for mass and charge transfer.

Fig. 3 shows the plots between $(\log R_{corr}/T)$ versus $(1/T)$ for 316 SS in free 2MHCl solution and when containing 225 ppm of three EDA molecules. Straight lines were acquired intercept equal to $[\log (R/Nh - \Delta S^*/2.303R)]$

The values of ΔH^* were determined from the slopes of straight lines ($-\Delta H^*/2.303 R$) and equals to $24.98 \text{ KJ mol}^{-1}$ in free 2M HCl and equal $34.46, 40.21$ and $42.12 \text{ KJ mol}^{-1}$ for molecules EDA1, EDA2 and EDA3 respectively. The positive values of ΔH^* elucidated that the endothermic nature of the dissolution process. This confirms that the dissolution of 316SS is difficult in the presence of EDA molecules.

The values of ΔS^* were assigned determined from the intercept of straight lines $[\log (R/Nh - \Delta S^*/2.303R)]$ and equals to $-38.42 \text{ J mol}^{-1}\text{K}^{-1}$ in free 2M HCl and equal $-42.72, -46.83$ and $-49.76 \text{ J mol}^{-1}\text{K}^{-1}$ for molecules EDA1, EDA2 and EDA3 respectively, The negative sign of ΔS^* demonstrates that the activated complex in the rate determination step symbolizes combination rather than disengagement reversed that more order takes place, going from reactant to activate complex.

3.5. EDA as pitting corrosion inhibitors

The PDAP measurements were utilized to confirm that the EDA molecules act as pitting inhibitors, Fig.5 displays the PDAP curves for 316 SS in 2.0MHCl +1.0MNaCl containing different

concentricity of EDA3 at scan rate 0.5 mVs^{-1} as an example of the investigated EDA molecules. The same figures were acquired in the case EDA1 and EDA2 molecules. The low scan rate to authorize pitting to begin at lesser noble potentials [26]

Inspection of the PDAP curves, it obvious that no any anodic peaks in the anodic scan owing to the forming of adhesive film on the surface of 316 SS. By examining the PDAP curves, we can observe that there are no anodic peaks in the anode scan, due to the chemical constitution of 316 SS contains Fe, Ni, Cr Mo and other elements, which leads to the formation of an adhesive film on the surface of 316 SS.

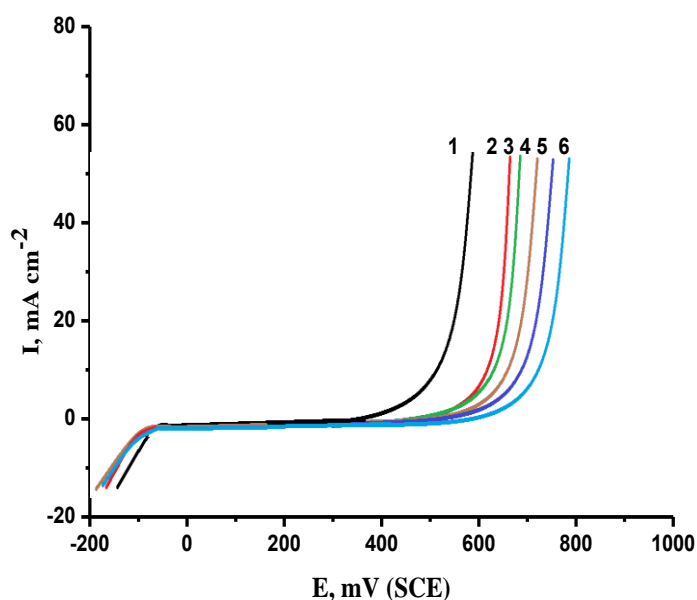


Figure 4. PDAP curves of 316 SS in 2.0M HCl + 1.0M NaCl solutions containing various concentrations of EDA3 at scan rate 1 mV s^{-1} . 1) 0.00 ppm EDA3 2) 25 ppm EDA3 3) 75 ppm EDA3 4) 125 ppm EDA3 5) 175 ppm EDA3 6) 225 ppm EDA3

As the potential increases, the current remains unchanged even at certain potential the current increase quickly due to the devastation of the adhesive film and beginning of the pitting attack. This potential is known as the pitting potential ($E_{\text{pit.}}$) [27,28]. As the concentricity of EDA molecule increases, $E_{\text{pit.}}$ values are transferred into the positive trend. This behavior demonstrates that EDA molecules inhibit the pitting corrosion of 316SS in chloride including solution.

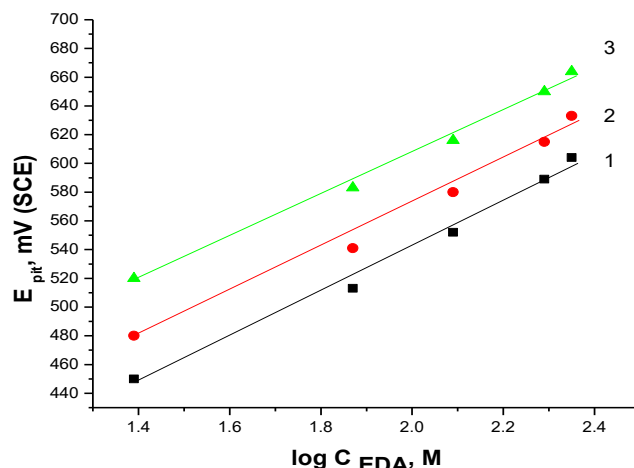


Figure 5. The relationship between E_{pit} and $\log C_{EDA}$ for 316 SS in 2M HCl + 1MNaCl solutions containing various concentrations of EDA molecules. 1)EDA1 2) EDA 2 3) EDA3

Fig .5 represents the relation between the $E_{pitt.}$ and the logarithmic of concentricity of EDA molecules. This relationship gives straight lines according the subsequent equation [27,28].

$$E_{pitt.} = A + B \log C_{EDA} \tag{5}$$

Where A and B are constants depending on the kind of the metal or alloy used and the additives applied. Clearly, from the Fig.6, with increasing the concentricity of EDA molecules, $E_{pitt.}$, is moved to a more noble trend. This confirm that the pitting corrosion of 316 SS is inhibited in the presence of EDA molecule.

3.3. Electrochemical impedance spectroscopy tests

Nyquist plot of CS 316 immersed in 2 M HCl solution in the absence and presence of the inhibitor are shown in the Fig.6. The diameter of the semicircle loop increases with increase in the inhibitor concentration. The impedance parameters such as solution resistance (R_s), charge transfer resistance (R_{ct}), double layer capacitance (C_{dl}) and percentage efficiency (%IE) are depicted in Table 3.

Inhibition efficiency and double layer capacitance were calculated by using the next equations :

$$\%IE = [1 - R_{ct (f)} / R_{ct (in)}] \times 100 \tag{6}$$

$$C_{dl} = 1/2\pi f_{max} R_{ct} \tag{7}$$

Where $R_{ct (f)}$ and $R_{ct (in)}$ are the charge transfer resistance before and after the addition of EDA, f_{max} is the frequency, at which imaginary components of the impedance reaches to maximum value.

EIS data revealed that charge transfer value increased from 170 to 1430 $\Omega \text{ cm}^2$, 170-1825 and 170-1910 $\Omega \text{ cm}^2$ for EDA1, EDA2 and EDA3 respectively, and double layer capacitance decreased from 128.2 to 2.7 $\mu\text{F. cm}^2$ with the increase in the amount of EDA concentration. Increase in R_{ct} value is because of the active components of the EDA hinders the corrosion rate through interfering the charge transfer process by blocking active sites of the 316SS surface in acid media under consideration. The downward trend of C_{dl} value could be connected to the decrease in the local dielectric constants arising from the displacement of water molecule on the 316SS surface by organic moieties present in the EDA

compounds [29,30]. The values of %P decreases in the following sequence: EDA3 > EDA2 > EDA1. This is constituent with the values obtained from GAP tests

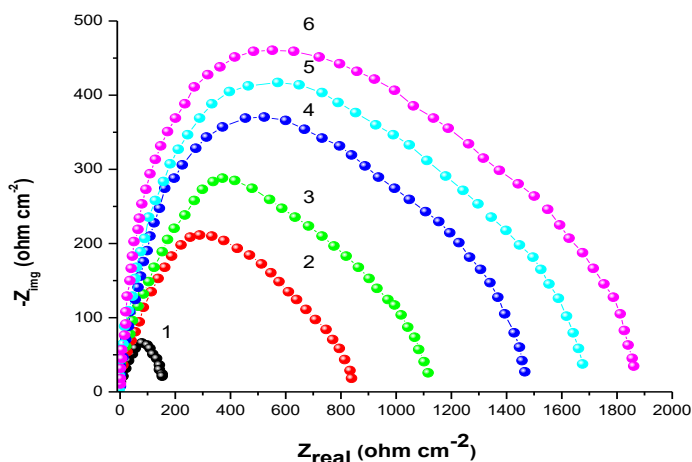


Figure 6. Nyquist plots of plots for corrosion of 316 SS in free 2M HCl and in the presence of some concentrations of EDA3 at 300K 1) 0.00 ppmEDA3 2) 25 ppmEDA3 3) 75 ppmEDA3 4) 125 ppmEDA3 5)175 ppmEDA3 6)225ppmEDA3

Table 3. EIS parameters of 316L SS in free 2M HCl solution and including some concentrations of EDA molecules

EDA Conc.	R_s	C_{dl} , $\mu F. cm^2$	R_{ct} , Ωcm^2	%P
2MHCl	12	128.2	170	-
<u>2MHCl+ EDA1</u>				
25 ppm	14	13.4	620	72.58
75 ppm	16	11.8	690	75.36
125 ppm	19	9.6	740	77.03
175 ppm	21	8.8	1055	83.88
225ppm	23	8.2	1430	88.11
<u>2MHCl+ EDA 2</u>				
25 ppm	13	12.8	685	75.18
75 ppm	15	9.6	805	78.88
125 ppm	18	7.8	1010	83.17
175 ppm	23	6.2	1360	87.50
225ppm	22	5.2	1825	90.68
<u>2MHCl+ EDA3</u>				
25 ppm	16	11.4	845	79.88
75 ppm	18	7.2	1200	85.83
125 ppm	20	5.8	1395	89.24
175 ppm	22	3.6	1720	90.11
225ppm	25	2.7	1910	91.99

3.5. Surface morphology

Fig.8 (A to D) represents the scanning electron micrographs of 316 SS surfaces after being immersed in free 2.0 M HCl solution alone and with 225 ppm of EDA molecules. The electrodes are immersed two hours in the examined solutions and subjected to GAP measurements. It is noticed that from Fig. 8A, the surface of 316SS is corroded after being immersed in a 2MHCl solution, and the presence of etched grain boundaries was observed, indicating corrosion of the 316SS. In the presence of three molecules of EDA in Fig (B, C and D) the surface of 316 SS was improved and some corrosion sites were removed.

The improving of the surface in the presence DEDA3 is more than EDA2 and EDA1. This is consistent with the inhibitory efficacy of the examined EDA molecules. The presence of EDA molecules construct an adsorbed film that prevent the arrival of aggressive solution to the surface of 316SS, Hence the corroded area on the 316SS surface is covered with the inhibitor. Among all the electrochemical techniques used, it was found that the: EDA3 molecule is more %P and has less corrosion attack and a good adsorbent film on the surface of 31SS. The adsorbent film in the case of EDA2 molecule has less protection than EDA3 molecule but more adhesive than EDA1 molecule.

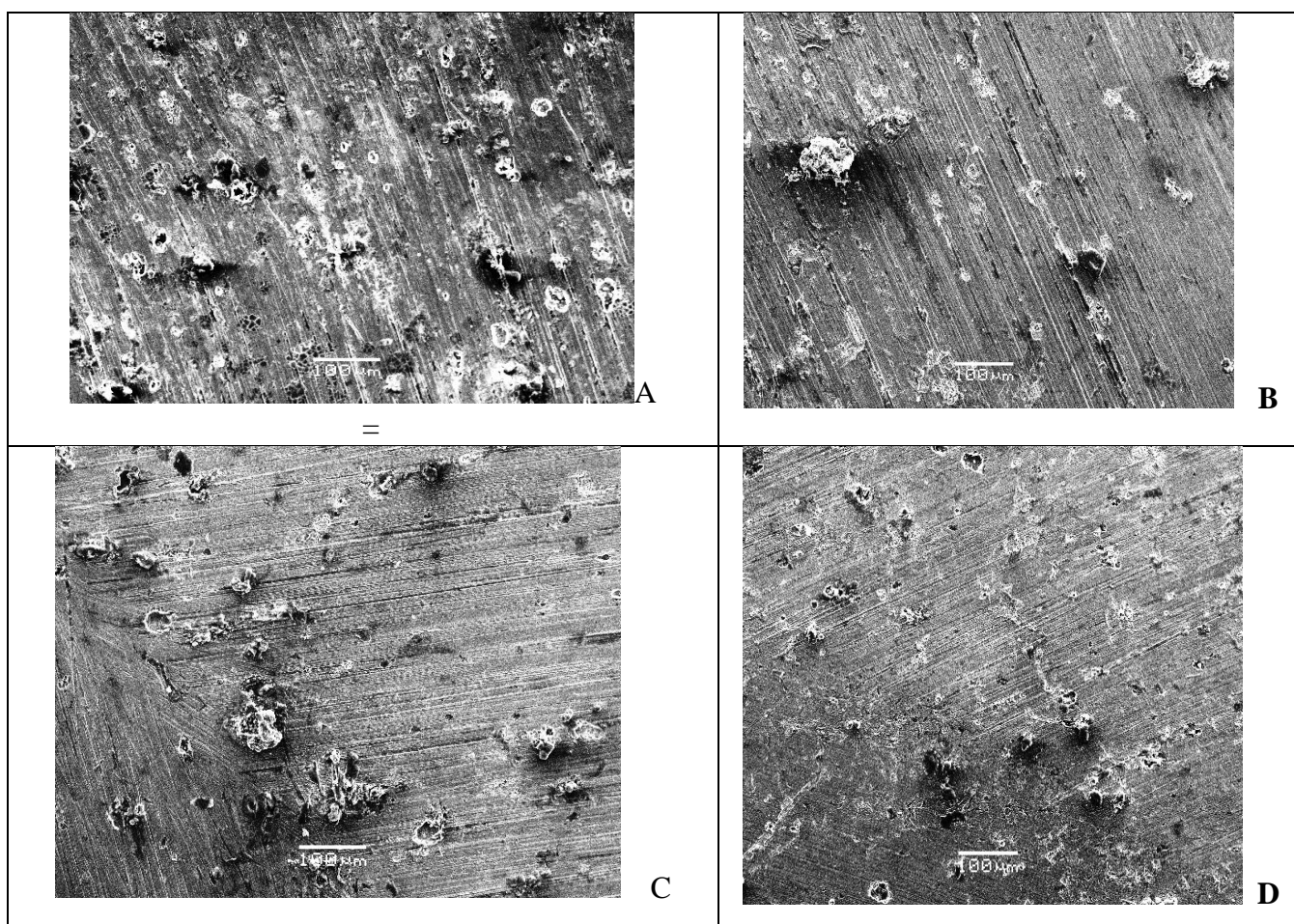


Figure 8. SEM micrographs (x500) of 316 surface after immersion in (a) in 2.0 M HCl. (b) 2.0 M HCl + 225 ppm of the EAD1 (c) 2.0 M HCl + 225 ppm of the EAD2 d) 2.0 M HCl + 225 ppm of the EAD3 using GAP tests

3.6. Adsorption isotherm and the inhibition mechanism

All the electrochemical tests used and surface morphology by SEM confirm the inhibitory effect of EDA molecules toward the corrosion of 316SS in 2M HCl solutions. This evidenced by the decrease of I_{corr} , R_{ct} , and the shift of E_{pit} , to more noble direction and thus the %P increases. The inhibiting potency of EDA molecules was mainly dependent on their adsorption on the surface of 316 SS. The adsorption operation is a interchange process between the EDA in aqueous solution and the number of H_2O molecules (z) adsorbed on the surface of 316SS.



Where, α is the size ratio that is the number of water molecules interchanged by one EDA molecule.

To find the appropriate adsorption isotherm, the values of θ are inserted into some isotherms. We found that the adequate isotherm is the Temkin isotherm according to the next equation [31]:

$$\ln \theta = \ln KC_{EDA} \tag{9}$$

The logarithmic form of this equation is :

$$\theta = \left[\frac{2303}{\alpha} \right] \log K_{ads} + \left[\frac{2303}{\alpha} \right] \log C_{EDA} \tag{10}$$

where K_{ads} is the equilibrium constant of the adsorption reaction, C is the concentration of EDA molecules and α is the interaction parameter

Fig.9 displays the Temkin plots (θ and $\log C_{EDA}$) for adsorption of EDA molecules on the 316SS surface in 2.0 M HCl solutions at 300 K. This relation gave straight lines demonstrated that the adsorption of EDA molecules on the 316 SS surface obeys Temkin isotherm. This isotherm is utilized in the ideal state of physical and chemical adsorption on a smooth surface with non-interaction between the adsorbed particles.

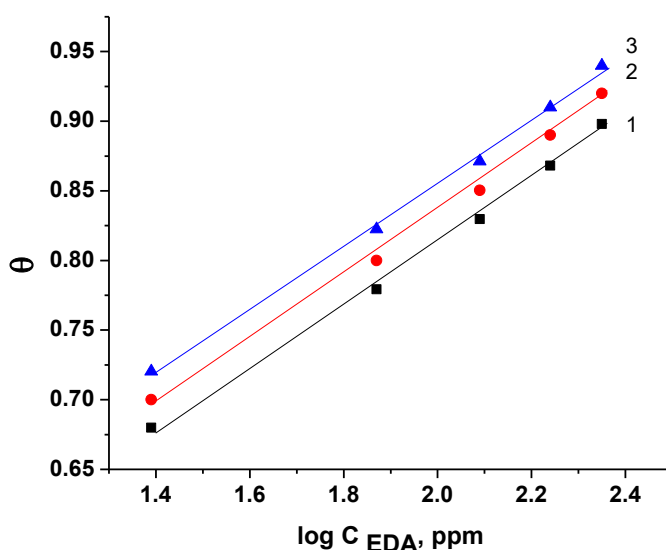


Figure 9. The relationship between θ and $\log C_{EDA}$ for 316 SS in 2.0 M HCl solutions containing various concentrations of EDA molecules. 1) EDA1 2) EDA2 3) EDA3

The free energy of adsorption ΔG_{ads}^* can be determined from the values of K_{ads} by applying the next equation

$$55.5 K_{\text{ads}} = \exp(-\Delta G_{\text{ads}}^*/RT) \quad (11)$$

The numerical value 55.5 is the concentration of water in mol L⁻¹

The computed value of K_{ads} are equal to 1.914, 1.963 and 2.013 for EDA1, EDA2 and EDA3, respectively. This high values elucidates the vigor adsorption of EDA molecules on the surface of 316 SS. The computed values of ΔG_{ads}^* for EDA molecules on the 316 SS surface are equal to -28.14, -30.22 and -31.13 kJ mol⁻¹ for EDA1, EDA2 and EDA3, respectively. The negative signs of ΔG_{ads}^* demonstrated that the adsorption process of EDA molecules on the 316SS surface is spontaneous.

The spontaneous adsorption of EDA molecules on the 316SS in 2MHCl solution depends on several functions such as the chemical structure of the molecule, the number of ethylene oxide unit present in its structure, the type of the stainless steel used and its chemical constitution, the concentration of the corrosive acidic solution and the temperature. The computed values of % P from all the techniques used increases with increasing the number of ethylene oxide present in the molecules. The values of %P decreases in the following sequence: EDA3 > EDA2 > EDA1

The inhibition strength of EDA molecules due to the formation of adsorbed film on the surface 316SS through the EO unit while the hydrocarbon parts protrude brush-like into the solution.

This behavior can be interpreted in light of the physical characteristics of the EDA molecules. These molecules have long hydrocarbon chains tend to wrap in water to reduce the contact area between the hydrophobic hydrocarbon chain and the water molecules [32].

Also, EDA molecules inhibits the pitting corrosion of 316 SS as revealed from PDAP measurements and this could be interpreted by the competitive adsorption between EDA molecules and Cl⁻ ions until the EDA molecule is the dominant than Cl⁻ ions. Therefore, the EDA overcome the Cl⁻ ions and thus reached the surface of 316 SS and form adsorbed film on its surface. Thus, the pitting attack is inhibited by moving the E_{pit} to more noble trend.

4. CONCLUSIONS

- a. EDA molecules act as efficacious inhibitor for corrosion of 316 SS in 2MHCl solution.
- b. The inhibition efficacy increases with increases the concentration of EDA molecules and the number of ethylene oxide unit and reduces at elevated temperatures.
- c. The inhibition effect of EDA due to its spontaneous adsorption on the 316 SS surface.
- d. The adsorption of EDA molecules on the 316SS surface according to Temkin's isotherm
- e. EDA molecules inhibit the pitting corrosion of 316 SS by moving the pitting potential to noble direction
- f. The inhibition efficacy from all electrochemical tests consistent with each other.

ACKNOWLEDGEMENT

This research was funded by the Deanship of Scientific Research at Princess Nourah bint Abdulrahman University through the Fasttrack Research Funding Program.

References

1. M. P. Asfia, M. Rezaei, G. Bahlakeh, *J. Mol. Liq.*, 315 (2020) 113679.
2. E. Alibakhshi, M. Ramezanzadeh, G. Bahlakeh, B. Ramezanzadeh, M. Mahdavian, M. Motamedi, *J. Mol. Liq.*, 255 (2018), 185.
3. M. Abdallah, B.A.AL Jahdaly, M. M. Salem A. Fawzy, A. A. Abdel Fattah, *J. Mater. Environ. Sci.*, 8 (2017)2599.
4. M. Abdallah, M. M. Salem, B.A.AL Jahdaly, M. I. Awad, E. Helal, A. S. Fouda, *Int. J. Electrochem. Sci.*, 12(2017)4543.
5. M. Abdallah, A. Al Bahir, H. M. Altass, A. Fawzy, N. El Guesmi, Arej S Al-Gorair, F. Benhiba, , I. Warad, A. Zarrouk, *J. Mol. Liq.*, 330 (2021) 115702.
6. M. Alahiane, R. Oukhribb, A. Berishacd, Y. A. Albrimia, R. A. Akboura, H. A. Oualide, H. Bourzib, A. Assabbane, A. Nahléf, M. Hamdania, *J. Mol. Liq.*, 328 (2021)115413.
7. M. Abdallah O. A. Hazazi, A.S. Fouda, A. Abdel-Fatah, *Prot. Met. Phys. Chem. Surf.*, 51 (2015) 473.
8. M. Abdallah, A.S. Fouda S.M. Al-Ashry, *Zastita Materijala* , 49 (2008) 22.
9. R. T. Loto, T. Morenikeji, A. Charles, *Chem. Data Collec.* 26 (2020) 100349
10. A.S. Fouda, M. Abdallah, S.M. Al-Ashry, A.A. Abdel-Fattah, *Desalination*, 250 (2010)538-543.
11. M. Taliban , K. Raeissi, M. Atapour , B. M. Fernández-Pérez, A. Betancor-Abreu, I. Llorente S. Fajardo, Z. Salarvand , S. Meghdadi , M. Amirnasr, R. M. Souto, *Corros. Sci.*, 160 (2019) 108130
12. M. Abdallah, *Mater Chem. Phys.*, 82 (2003)786.
13. M. Abdallah, *Corros. Sci.*, 44 (2002).717.
14. M. Abdallah, M. Alfakeer, Amal M. Alonazi, Salih S. Al-Juaid , *Int. J. Electrochem. Sci.*, 14 (2019)10227.
15. S. Safak, B. Duran, A. Yurt and G. Turkoglu, *Corros.Sci.*, 54(2012)251-259.
16. Fawzy, M. Abdallah, M. Alfakeer, H. M. Ali., *Int. J. Electrochem. Sci.*, 14 (2019) 2063.
17. M. Abdallah, M.A. Hegazy, M. Alfakeer, H. Ahmed, *Green Chem. Lett. Rev.*, 11(4)(2018)457.
18. A. Fawzy, M. Abdallah, I. A. Zaafarany, S. A. Ahmed, I. I. Althagafi, *J. Mol. Liq.*, 265 (2018) 276
19. M. Sobhi, R. El-Sayed, M. Abdallah, *Chem. Eng. Comm.*, 203(2016)758.
20. F. Hanna, G.M. Sherbini, Y. Barakat, *Br. Corros. J.*, 24 (1989) 269.
21. H. Amar, A. Tounsi, A. Makayssi, A. Derja, J. Benzamorff, A. Outzourhit, *Corros.Sci.*, 49(2007) 2936.
22. M.A. Migahed, E.M.S., Azzam, S.M.I. Morsy, *Corros. Sci.*, 51(2009) 1636-1644.
23. O. L. Riggs Jr. and R. M. Hurd, *Corrosion*, 23 (1967) 252.
24. K. J. Laidler, *Chemical Kinetics*, Mc Graw Hill Publishing Company Ltd., 1965.
25. M. Abdallah, B. H. Asghar, I. Zaafarany, M. Sobhi, *Prot. Met. Phys. Chem. Surf.*, 49(4) (2013) 485.
26. M. Abdallah, A.I. Mead, *Annali Di Chimica*, 83 (1994) 424.
27. M. Abdallah, H.M. Altass, Arej S Al-Gorier, Jabir H. Al-Fahmi, K.A. Soliman, *J. Mol. Liq.*, 323(2021)115036.
28. M. Abdallah, I. Zaafarany. S.O. Al-Karane and A. A. Abd El-Fattah, *Arab. Chem*, 5 (2012), 225.
29. M. Alfakeer M. Abdallah, R.S. Abdel Hameed, *Prot. Met. Phys. Chem. Surf.*, 56 (2020) 225.
30. M. Sobhi, R. El-Sayed, M. Abdallah, *J. Surf. Deter.*, 16(2013)937-946.
31. M. Abdallah, M. Sobhi, H.M. Altass, *J. Mol. Liq.*, 223(2016)1143-1150.
32. G. Schmitt. Proc. 6th Enrop. Symp. Corros. Inhibitors Ferrara, Italy (1985) separate paper